Journal of Applied Polymer Science

# Platelet lysate and adipose mesenchymal stromal cells on silk fibroin nonwoven mats for wound healing

**Chlapanidas Theodora,[1] Perteghella Sara,[1] Faragò Silvio,[2] Boschi Alessandra,[2] Tripodo Giuseppe,[1] Vigani Barbara,[1] Crivelli Barbara,[1] Renzi Sabrina,[3] Dotti Silvia,[3] Preda Stefania,[4] Marazzi Mario,[5] Torre Maria Luisa,[1] Ferrari Maura[3]**

[1]Department of Drug Sciences, Medicinal Chemistry and Technology Section, University of Pavia, Pavia 27100, Italy
[2]Innovhub, Stazioni Sperimentali per L'industria, Silk Division, Milan 20133, Italy
[3]Cell Culture Center, Istituto Zooprofilattico Sperimentale della Lombardia e dell'Emilia Romagna, Brescia 25124, Italy
[4]Department of Drug Sciences, Pharmacology Section, University of Pavia, Pavia 27100, Italy
[5]Struttura Semplice Tissue Therapy, Niguarda Ca' Granda Hospital, Milan 20162, Italy
Correspondence to: S. Perteghella (E-mail: sara.perteghella@unipv.it)

**ABSTRACT:** In this work platelet lysate (PL) and adipose-derived mesenchymal stromal cells (ASCs) seeded on nonwoven fibroin mats were *in vitro* and *in vivo* evaluated for tissue regenerative applications. Nonwoven mats obtained by a large scale water entanglement technique were characterized for their physico-chemical properties. Results indicated a high purity of fibroin fibers, their stability after sterilization process and appropriate technological properties suitable for tissue engineering. Moreover, the scaffolds *in vitro* supported adhesion and migration of ASCs and the presence of PL improved the cell proliferation. The products were then applied on epithelial/dermal wounds carried out on the dorsal surface of rabbit: the skin reparative process was solved in 9 days, with a completely *restitutio ad integrum* of the epithelium in animals treated with PL alone; ASCs did not further improve the wound healing. © 2015 Wiley Periodicals, Inc. J. Appl. Polym. Sci. **2016**, *133*, 42942.

**KEYWORDS:** biomaterials; fibers; properties and characterization

Received 30 June 2015; accepted 15 September 2015
**DOI: 10.1002/app.42942**

## INTRODUCTION

Healing of some wounds, such as pressure, diabetic, and venous ulcers, remains an unresolved problem with high costs for the healthcare.[1] In tissue repair, advanced therapy medicinal products (ATMPs), in particular tissue engineered ones, usefully support the conventional therapy when it fails. For the treatment of the wounds, different biomaterials have been proposed, based on natural polymers, such as polysaccharides (e.g., alginates, chitosan, and hyaluronic acid)[2–5] and proteins (e.g., collagen, silk fibroin, and gelatin) or synthetic polymers (the most common are polylactic acid, polyglycolic acid, poly-ε-caprolactone, and polyethylene glycol).[6–12] Despite the devices based on synthetic polymers show higher mechanical strength with respect to those composed by natural polymers, the latter are considered the first choice because of their biocompatibility, biodegradability, and similarity with extracellular matrix.[13] Among the plethora of natural polymers examined for wound healing applications, silk fibroin is a promising candidate.[14–20] In literature, silk fibroin has been proposed for tissue engineering and regenerative medicine, also combined with other polymers in different forms, including sponges, microparticles, films, hydrogels, and nonwoven mats.[21–27] In this context, silk fibroin nonwoven scaffolds are helpful devices for different cell support,[28–31] both *in vitro* and *in vivo*, because of their high surface area, rough morphology, tunable porosity, architecture/network similar to extracellular matrix, biocompatibility, suitable angiogenesis supporting properties, and biodegradability.[21,32,33] On the other side, a number of nonwoven materials from different starting polymers are present in literature and show specific behaviors. This kind of nonwoven mats are usually obtained by applying electrospinning techniques and, when used for wound healing application, the use of platelet lysate and/or mesenchymal stromal cell to drive the healing process is proposed, even if only a few example of these materials cold be found due to the novelty of the systems. For example, Schellenberg *et al.*, proposed the use 3D nonwoven fibrous materials based on polyvinylidene fluoride (PVDF). To this material, human

Additional Supporting Information may be found in the online version of this article.

mesenchymal stromal cells (MSCs) from adipose tissue, were seeded in parallel and their growth was studied.[34] In another study, aligned and random-oriented poly (3-hydroxybutyrate-*co*−3-hydroxyvalerate) PHBV nanofibrous scaffolds loaded with hydroxyhapatite (HA) nanoparticles were fabricated through electrospinning technique. Mesenchymal stem cells (MSCs) derived from rat bone marrow were used to investigate the effects of HA and orientation of fibers on cell proliferation and differentiation *in vitro*. This material exhibited significant effects on the repair of critical bone defects.[35] Shen *et al.* studied the effect of neurotrophin-3 (NT-3) on accelerating wound healing in the diabetic foot by improving human bone marrow MSC (hMSC) activation. The biomaterial which supported the application of NT-3 and hMSC was composed from 80% polylactic acid, 10% silk fibroin, and 10% collagen and obtained by electrospinning. They found that the NT-3-stimulated hMSCs in the biological tissue material significantly promoted angiogenesis in the feet of diabetic C57BL/6J mice and accelerated diabetic foot wound healing.[36]

For tissue regeneration, an effective tissue engineered product should contain: scaffold, cells, should be able to promote and/or sustain the healing process, and bioactive substances.[37] The main cells employed in wound healing are keratinocytes and fibroblasts,[38] but also various progenitor cells could effectively support the wound healing process[39,40]; in particular, adipose tissue is an ideal source of stromal cells[41] because of its abundance in the body[42] and its easy surgical retrieval. Moreover, adipose-derived stromal cells (ASCs) have the ability to differentiate in various cell lines,[43–49] to modulate the immune response,[50] to promote re-vascularization[51,52] and to deliver loaded drugs.[53] Navone *et al.* (2014) produced silk fibroin patches by electrospinning and observed a skin regeneration in 10 days in a murine model, using scaffolds both cellularized with ASCs or decellularized.[54]

The platelet lysate (PL), obtained after disruption via −80°C freeze-thawing of platelet concentrates, has been applied as therapeutic agent for wound healing because it releases growth factors and bioactive substances able to regulate cellular mechanisms.[55,56] *In vitro* studies demonstrated that PL stimulates the keratinocyte migration through a calcium and p38-dependent mechanism,[57] actives an inflammatory cascade and has antimicrobial properties.[58] Furthermore, fibroblasts were activated after culture supplemented with PL modifying proteins principally related to stress response, metabolism, and cytoskeleton.[59] PL was effectively loaded in calcium alginate particles[60] or dressings based on hyaluronic acid sodium salt and glycine.[61] Finally, the combined use of bone marrow stromal cells and PL on fibrin or collagen scaffolds was evaluated in a sheep model, promoting the new bone formation.[62]

The technological development of a pharmaceutical grade scaffold is a prerequisite for its subsequent use in tissue engineering as well as its large scale production to allow reasonable costs to the end user. In this work, silk fibroin nonwoven scaffolds, industrially produced, were characterized to verify their suitability for tissue engineering and regenerative medicine applications. Therefore, for the first time, ASCs and PL were loaded on silk fibroin nonwoven mats and the capability of the construct to repair skin wounds was evaluated *in vivo* (rabbit model).

## MATERIALS AND METHODS

### Preparation of Fibroin Nonwoven Mat

Silk fibroin scaffolds were produced by the water entanglement method.[63] Briefly, cocoon fibers were cut, placed in distilled water, and autoclaved (110–135°C, 2 atm) for 1 h in order to eliminate sericins.[64] Fibroin fibers were washed two times with distilled water at 60°C and dried, parallelized using a carding/combing laboratory machine and cut with a ceramic blade in order to obtain samples of about 40 mm in length. The carding apparatus was set to produce three types of fiber pads differing in weight/surface area ratio, named as SF1 (thin), SF2 (medium), and SF3 (thick).

Nonwoven mats were obtained by entanglement using high-pressure water jets (80 bar), and dried at 140°C. The weight/surface area ratio and the apparent density of the obtained scaffolds (weight/volume ratio), were valued after accurately cutting 1 cm × 1 cm samples and calculation of the scaffold thickness by a certified micrometer. Furthermore, the porosity % ($\varepsilon$) of the scaffolds has been calculated by applying eq.[65]:

$$\varepsilon = \left[1 - \left(\frac{\delta}{\delta_0}\right)\right] * 100 \quad (1)$$

where $\delta$ is the apparent density of the scaffolds and $\delta_0$ is the bulk density of the silk fibroin (1.25 g $cm^{-3}$).

Fibroin nonwoven mats were sterilized by heat in a Systec V-65 autoclave (121°C for 20 min, drying 10 min) or by gamma rays irradiation (60 kGy). A microbial test was performed after sterilization processes: scaffolds were incubated for 7 days in Dulbecco's modified Eagle's medium (DMEM) at 37°C, 5% $CO_2$: after this period, 5 mL of the supernatant were inserted into an adequate bottle and analyzed using BacT/ALERT 3D system to detect bacteria and fungi.

### Scanning Electron Microscopy/Energy Dispersive X-ray (SEM/EDX) Analysis of Nonwoven Scaffold

After sterilization, fibroin nonwoven scaffolds (SF1 and SF3 mats) were analyzed using a scanning electron microscope (Mira 3, Tescan) operating at 15 kV, retrodiffused electron signal. To detect the possible heavy metal contamination from technological process, EDX analysis was carried out by the iXRF system and EDS-2004 system for revelation.

### Fourier Transform Infrared Spectroscopy (FTIR)

Before and after sterilization, fibroin nonwoven mats were analyzed by FTIR on a Bruker Alpha-E spectrometer equipped with a MIRacle™ attenuated total reflection Diamond crystal cell in reflection mode. Background measurements were taken twice with an empty cell and subtracted from the sample readings. The FTIR spectra in the absorbance mode were obtained in the spectral regions of 375–4000 $cm^{-1}$. Each spectrum of the samples was acquired by accumulation of 24 scans with a resolution of 4 $cm^{-1}$. FTIR is a useful tool to monitor the silk fibroin conformation changes. In fact, silk fibroin can exist at the three molecular conformations: *Silk I*, a mix of random coil, α-helix and *β*-turn, *Silk II*, a *β*-sheet structure, and *Silk III*, an α-helix

structure in water/air interface.[66,67] For proteins and peptides, relevant spectral regions are the so-called Amide I (1700–1600 $cm^{-1}$, corresponding to C═O stretching), Amide II (1540–1520 $cm^{-1}$, corresponding to N—H bending and C—N stretching), and Amide III (1300–1220 $cm^{-1}$, indicating C—N stretching and C═O vibration).[68,69] A fibroin secondary structure is related to specific shifts of the Amide I, II and III peaks: for Amide I, a value of ~1650 $cm^{-1}$ is linked to a random coil structure, whereas a value of ~1630 $cm^{-1}$ corresponds to a $\beta$-sheet structure; for amide II, wavenumbers of ~1540 $cm^{-1}$ and ~1520 $cm^{-1}$ correspond to random coil and $\beta$-sheet structure, respectively; finally, for amide III, peaks at ~1230 $cm^{-1}$ and ~1270 $cm^{-1}$ indicate, respectively random coil and $\beta$-sheet structure.[69]

### Differential Scanning Calorimetry Analysis (DSC)

Before and after sterilization, fibroin nonwoven mats were analyzed by a Mettler TA30 differential scanning calorimeter. Thermal scanning was carried out on 1.2–2.4 mg of each sample under nitrogen (temperature range: 20–500°C, rate: 10°C $min^{-1}$) on a single course.

### Mechanical Measurements

Samples of fibroin non-woven scaffold (30 cm × 5 cm) were secured between two 20-cm distant clamps of a tension tester (5900 Series, Instron, Italy); the tensile test was conducted in a conditioning room with temperature 20°C, humidity 60% and with stretching speed of 10 cm $min^{-1}$. The experiments were performed as a function of sample orientation: parallel orientation means that the tensile force direction follows the same orientation of the fibers as emerging from carding/combing machine, while perpendicular orientation indicates that the tensile force direction has been applied perpendicularly to the fiber orientation. For each sample, five replicates were carried out. The output variables were strength at break (MPa) and elongation at break (%) with respect to the starting length.

### Animals

Adipose tissue samples were collected from 20 adult rabbits (mean weight: 4 kg) at abattoir immediately after slaughtering. Blood samples collection [for Platelet Lysate (PL) preparation] was performed at IZSLER facilities using 10 male adult SPF New Zealand rabbits (mean weight: 3 kg). Animals were housed with water and feeding *ad libitum*. They were allocated in single cage.

All the medical procedures were performed following Laboratory Animals Welfare National Directive. Furthermore, in order to reduce the number of considered animals during the experimental design, as described in National Directive, the same rabbits were included in the therapeutic procedures.

### Isolation and Expansion of ASCs

About 20 g of each adipose tissue were immersed in phosphate buffered solution (PBS), containing penicillin 5000 IU $mL^{-1}$, streptomycin 625 $\mu g$ $mL^{-1}$, and amphotericin B 51 $\mu g$ $mL^{-1}$ (all purchased from Squibb, Roma, Italy), and carried to the laboratory.

All the procedures were performed in laminar flow hood, class II. Initially, tissue was mechanically minced and subsequently treated with 7.5 mg $mL^{-1}$ type I collagenase (Sigma Aldrich, Milano, Italy) at 37°C for 1 h in mild shake conditions. At the end of the incubation period, 10% v/v fetal bovine serum (FBS, Euroclone, Milano, Italy) was added to each cell suspension, in order to inhibit enzyme action. Cell suspension was filtered through a 50-μm nylon mesh and centrifuged at 250*g* for 10 min at 20°C. Cell pellet was diluted in NH Expansion Medium (Miltenyi Biotec, Bologna, Italy) containing 1000 IU $mL^{-1}$ penicillin and 100 μg $mL^{-1}$ streptomycin. Finally, cells were counted with Cellometer Automated Cell Counters (Nexcelom Bioscience, USA) with Trypan Blue (Sigma–Aldrich, Italy) staining. The 5 × $10^4$ cells/$cm^2$ were resuspended in culture medium, seeded in tissue culture flasks and incubated at 37°C in 5% $CO_2$. The medium was changed after 48 h and then every third day. Subcultures were performed when cells reached 80–90% confluence. To detach cell monolayer, cells were treated with a solution composed by sodium chloride (80 μg $mL^{-1}$), potassium chloride (4 μg $mL^{-1}$), glucose (10 μg $mL^{-1}$), sodium bicarbonate (3.5 μg $mL^{-1}$), phenol red (1.8 μL $mL^{-1}$), trypsin (50 μL $mL^{-1}$), EDTA (2.5 μg $mL^{-1}$) for 5 min at 37°C (all purchased from Euroclone). Cells were splitted at 1:3 ratio in complete culture medium and incubated at 37°C in 5% $CO_2$. A maximum of three serial passages were carried out and a total of about 20 × $10^6$ cells were obtained, with about 90% viability.

Microbiological controls were performed at each medium change and when cells were expanded; in particular 500 μL of cell suspension were inoculated in Tryptone Soy Broth and Thioglycolate.

### Platelet Lysate (PL) Preparation

The PL preparation was performed according to Luengo Gimeno *et al.* (2006).[70] About 40 mL of whole venous blood of 20 adult rabbit were collected into 5 mL tubes containing 100 IU $mL^{-1}$ heparin (Sigma Aldrich, Milan, Italy). Blood was centrifuged at 72 × *g* for 15 min at 4°C; the plasma, represented by the superior layer, was centrifuged at 1000 × *g* for 10 min at 4°C. Platelet pellet was collected and diluted in 4 mL plasma; cells were counted by the hematology analyzer CELL-DYN 3500R (Abbott, Latina, Italy). Finally, the suspension was cryopreserved at −80°C overnight, in order to permit platelets lyses. The following day, platelets suspension was rapidly thawed in a 37°C water bath, then it was three times centrifuged (1000 × *g*, 10 min, 4°C), in order to discard platelet fragments (pellet fraction). PL had a concentration of 0.25 × $10^6$ platelets/mL and was sterile distributed in 2 mL doses and stored at −80°C until use. Microbiological controls were performed before sample freezing, in particular 500 μL suspension were inoculated in Tryptone Soy Broth and Thioglycolate.

### *In Vitro* Studies

Silk fibroin nonwoven mats (SF1) were minced in 1 × 1 $cm^2$ and sterilized by autoclave stream (121°C, 15 min). About 50 μL PL (14 × $10^3$ platelets) and 100 × $10^3$ ASCs were dripped on scaffold surface and then medium was added. ASCs were cultured until 14 days, changing medium every 72 h. The same experiments were performed without PL, in medium

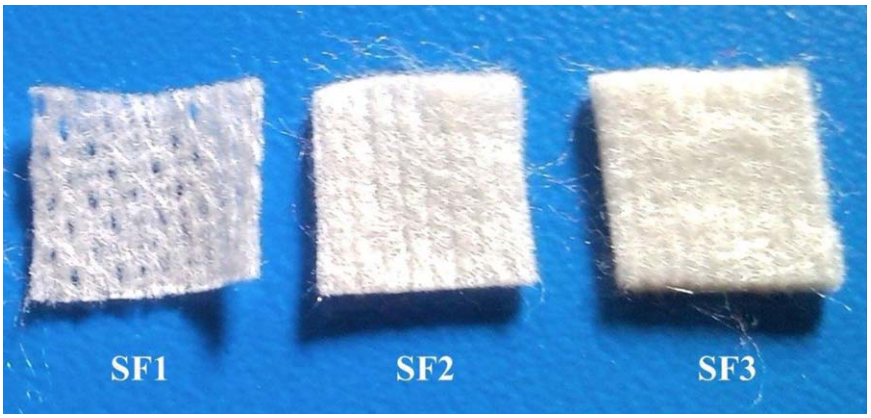


**Figure 1.** Optical photography of SF1 (thin), SF2 (medium), or SF3 (thick) mats showing the macroscopic aspect of the materials such as the orientation of the fibers and the thickness. [Color figure can be viewed in the online issue, which is available at wileyonlinelibrary.com.]

supplemented with FBS as a control. Each condition was tested in triplicate.

Cell proliferation was assessed by MTT assay. Briefly, culture medium was discarded and 100 µL of 3-(4,5-dimethylthiazol-2-yl)−2,5-diphenyltetrazolium bromide (MTT) solution (0.5 mg $mL^{-1}$) were added. After 3 h at 37°C, the medium was removed and substituted with 100 µL of dimethyl sulfoxide (DMSO). The optical density was measured at 570 and 670 nm (reference wavelength).

After the 14-day culture, ASCs were fixed with three different subsequent solutions: glutaraldehyde 2% in DMEM, glutaraldehyde 2% in cacodylate buffer 0.1M and cacodylate buffer 0.1M for 30 min each. Cells were treated with ethanol solution at different concentration (30, 50, 70, 90, and 100%) for 15 min each. Then scaffolds were investigated with scanning electron microscopy (SEM). For transmission electron microcopy (TEM) analysis, samples were cut and fixed first with glutaraldehyde 2.5% in cacodylate buffer 0.1*M*, then with osmium tetroxide 0.1% and finally with alcohols. The scaffold was included in Epon 812/Araldite resin before being sectioned using Ultracut S Ultramicrotome. The ultrathin sections were observed for transmission electron microscopy with a JEOL JEM 1200 EX instrument.

### *In Vivo* Studies

Ten animals were divided in three groups: group 1 and group 2 were composed by four subjects each, while group 3 by two rabbits. Group 1 was treated with SF1 and PL alone, group 2 with SF1, ASCs, and PL, finally group 3 (control) was treated with SF1 in physiological solution (B. Braun Melsungen AG, Milan, Italy).

Silk fibroin nonwoven mats were minced in 4 × 4 $cm^2$ fragments and sterilized by autoclave steam. Scaffolds were soaked with 750 µL PL ($3 \times 10^5$ platelets/mL) alone or associated with ASCs ($2.5 \times 10^6$ cells $mL^{-1}$), respectively. Finally, scaffolds used in group 3, were soaked with 750 µL of sterile physiological solution.

All the medical procedures were performed with sedation and analgesia management. In particular, for each animal, an area of 6 $cm^2$ was identified on the dorsal surface, between thoracic and lumbar zone; this area was shaved. To avoid irritation event, 24 h after this procedure, the medical treatment was performed. First of all, each area was disinfected with chlorhexidine digluconate 4% (ICF S.r.l., Cremona, Italy) and animals received a mild sedation by a combination of acepromazine (0.2 mg $kg^{-1}$) and butorphanol (1 mg $kg^{-1}$) by subcutaneous route. A 2 × 2 $cm^2$ epithelial/dermal wound was carry out by a sterile lancet deep scrubbing. After this procedure, group 1 was treated with scaffold soaked with PL, otherwise scaffolds associated with PL and ASCs were applied to animals of group 2. All the animals received for 3 days an analgesic treatment based on a meloxicam (0.3 mg $kg^{-1}$, Boehringer Ingelheim, Milano, Italy) subcutaneous injection and no antibiotic was administrated. A daily observation of the animals was performed (physical examination) and each scaffold was changed every 72 h, with the same composition and dosage, for a total of three applications.

Before each treatment (time zero) and at three time points (3, 6, and 9 days), wounds were photographed; at the end of experiments, a score between 10 (starting wound) and 0 (complete wound healing) was given by independent expert operators ($n = 3$).

### Statistical Analysis

Statistical analyses were evaluated using a multifactor analysis of variance. Results of ASC proliferation were processed considering the time of culture and type of supplement (PL and serum) as fixed factor, and optical density as independent variable; wound healing scores evaluation was analyzed considering treatment (group 1, 2, and 3) and time (3, 6, and 9 days) as fixed factors.

**Table I.** Weight/Area Ratio, Thickness, and Porosity % of Three Different Fibroin Scaffolds ($n = 5$ for Each Sample)

| Scaffold | Weight/area ratio (g $m^{-2}$) | Thickness (mm) | Porosity % ($\varepsilon$) |
|---|---|---|---|
| SF1 | 41.3 ± 2.1 | 0.8 ± 0.1 | 95.9 ± 1.2 |
| SF2 | 79.1 ± 3.5 | 1.3 ± 0.2 | 95.1 ± 2.4 |
| SF3 | 123.5 ± 2.8 | 2.6 ± 0.1 | 96.2 ± 0.9 |

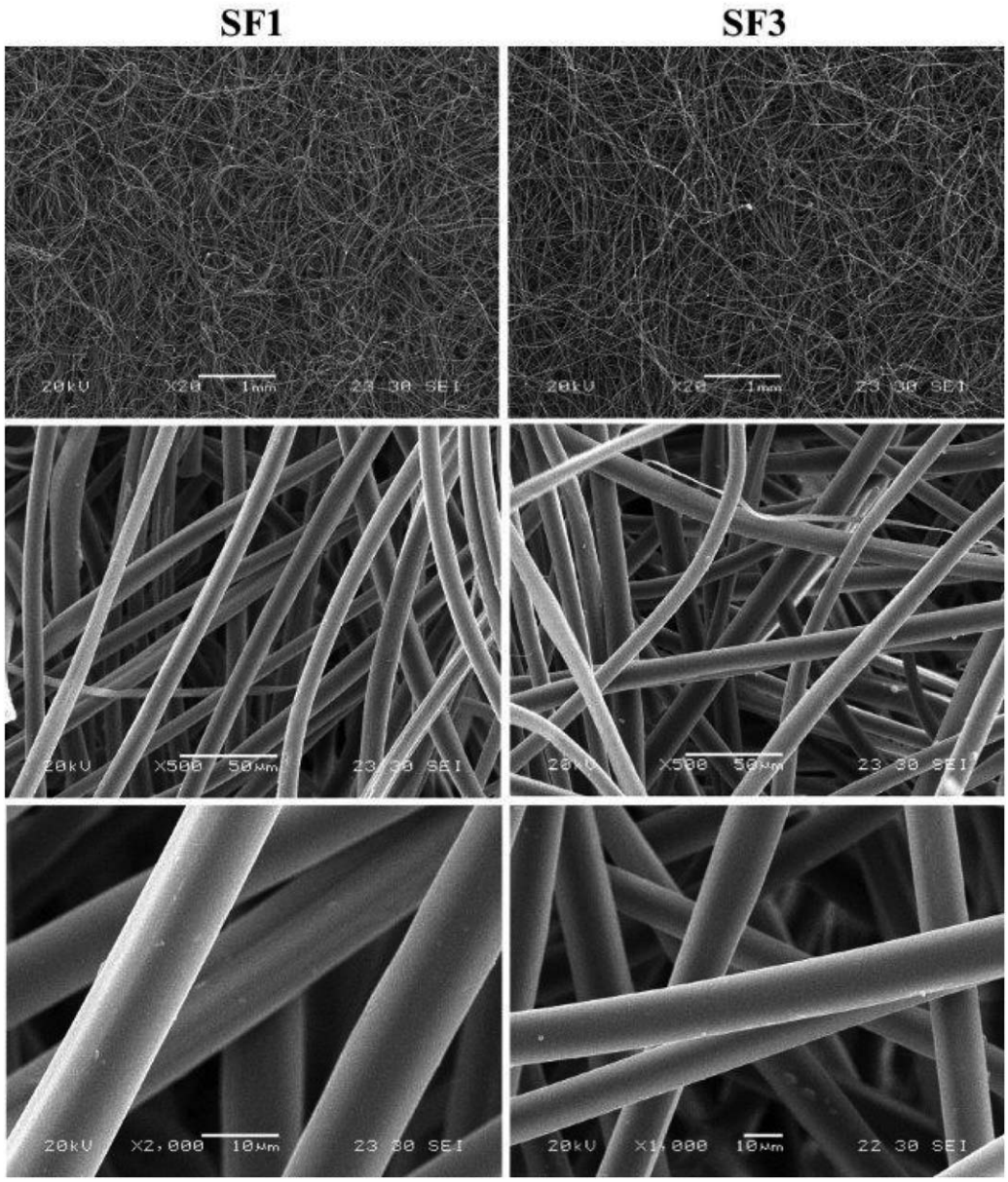


**Figure 2.** Scanning electron microphotographs of nonwoven mats at different magnifications, SF1 (left column) and SF3 (right column).

The differences between groups were analyzed with the *post hoc* LSD's test for multiple comparisons. The statistical significance was fixed at $P \leq 0.05$.

## RESULTS

### Technological Characterization of Silk Fibroin Nonwoven Mats

In this work, three different silk fibroin nonwoven mats were obtained by applying a large scale water entanglement method. Depending on the thickness, the obtained samples have been named as SF1 (thin), SF2 (medium), or SF3 (thick) (Figure 1).

The obtained nonwoven mats showed a weight/area ratio between 41.3 and 123.5 g $m^{-2}$, a thickness between 0.8 and 2.6 mm and a porosity between 95.9 and 96.2% (Table I).[71]

The three different silk fibroin nonwoven mats were macroscopically valued by optical photography (Figure 1). As from Figure 1, the fibers orientation and their spatial distribution did not result macroscopically influenced by the different mats thickness.

To better characterize the obtained mats, the SF1 and SF3 have been submitted to SEM investigation. The SEM analysis of samples (Figure 2) indicated that the microstructure was similar in mats with different weight/area ratios (41.3 and 123.5 g $m^{-2}$, respectively); both scaffolds showed a homogeneous aspect (Figure 2, top) and inter-fiber mesh distribution (Figure 2, center), with smooth surface, appreciable at higher magnification (Figure 2, bottom).

For *in vivo* applications, it was fundamental to verify that harmful contaminants were not presented as residues from the

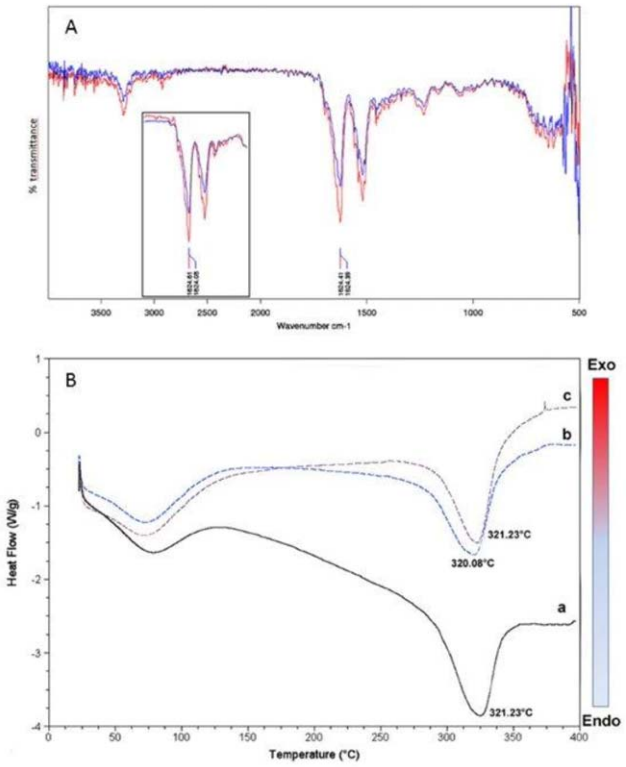


**Figure 3.** FTIR spectra and DSC patterns of SF1 mats. (A) FTIR spectra before (red) and after gamma-ray sterilization at 60 kGy (blue); inset: FTIR spectra before (red) and after autoclave sterilization (blue). (B) DSC patterns (a) before sterilization; (b) after autoclave sterilization; (c) after gamma-ray sterilization at 60 kGy. [Color figure can be viewed in the online issue, which is available at wileyonlinelibrary.com.]

processing method. EDX analysis of thin mats underlined the high purity of the nonwoven fibers: no contaminant heavy metals from water entanglement process were detected (see Supporting Information Figure S1).

The suitability of the production method was confirmed also by FTIR spectra performed on SF1. Fibroin nonwoven mat presented peaks at 1626 and 1518 $cm^{-1}$, respectively for Amide I and Amide II [Figure 3(A), red line]. After sterilization by both autoclaving or gamma rays irradiation, the FTIR analysis has been repeated to evaluate whether the sterilization method could affect the conformation of fibroin. FTIR spectra showed the same peaks of not sterilized samples (after heat sterilization 1626 and 1519 $cm^{-1}$, after gamma radiation 1627 and 1521 $cm^{-1}$, respectively for Amide I and Amide II).

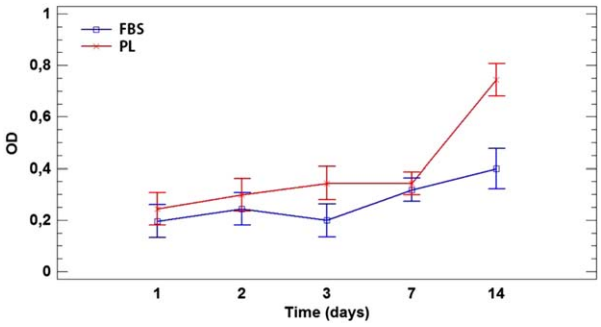


**Figure 4.** Mean values and 95.0% LSD intervals of optical density of ASCs on SF1 cultured until 14 days with PL or FBS (control). [Color figure can be viewed in the online issue, which is available at wileyonlinelibrary.com.]

DSC analysis showed, before and after sterilization of SF1 scaffold, an endothermic peak related to fibroin degradation at ~320°C [Figure 3(B)].

Mechanical properties of SF1 and SF3 were evaluated in terms of tensile strength and elongation at break; the fiber mat orientation and mat thickness showed a significant effect on mechanical properties, Table II. In fact, the thinnest sample (SF1) showed a tensile strength lower than SF3 mat both in parallel and perpendicular orientation, while elongation at break resulted similar.

On the basis of the technological characterization of mats that returned effective results for all the tested samples, SF1 was selected for the further *in vitro* and *in vivo* characterization since it resulted more easy to handle. Moreover, the reduced thickness would allow a faster oxygen, nutrients and metabolites diffusion.

### *In Vitro* Interaction of ASCs and Fibroin Mats

ASCs, isolated from intra-abdominal subcutaneous adipose tissues of adult SPF New Zealand rabbit, were seeded on SF1 surface and cells were cultured until 14 days to evaluate the ASCs attachment and migration into the biomaterial; the effect of PL on ASCs proliferation was considered. Being ASCs living cells, their seeding on the fibroin mats should be safety for the cell itself and promote their peculiar activities, e.g., the paracrine activity. MTT test results are reported in Figure 4 as optical density (mean values and 95.0% LSD intervals) during the culture time. These results, processed by a linear statistical model (ANOVA), evidenced that the OD depends on medium supplement ($P = 0.0001$) and culture time ($P < 0.0001$). In particular, in both cell culture conditions, the ASC proliferation increases

**Table II.** Tensile Strength and Elongation at Break % of SF1 and SF3 as a Function of Sample Orientation

| Sample | Tensile strength (MPa); parallel orientation | Elongation at break (%); parallel orientation | Tensile strength (MPa); perpendicular orientation | Elongation at break (%); perpendicular orientation |
|---|---|---|---|---|
| SF1 | 1.47 ± 0.15 | 29.43 ± 3.18 | 0.99 ± 0.08 | 65.75 ± 2.47 |
| SF3 | 2.14 ± 0.27 | 32.77 ± 2.72 | 1.30 ± 0.14 | 55.38 ± 2.96 |

Parallel orientation means that the tensile force direction follows the same orientation of the fibers as from carding/combing machine while perpendicular orientation indicates that the tensile force direction has been applied perpendicularly to the fiber orientation ($n = 5$).

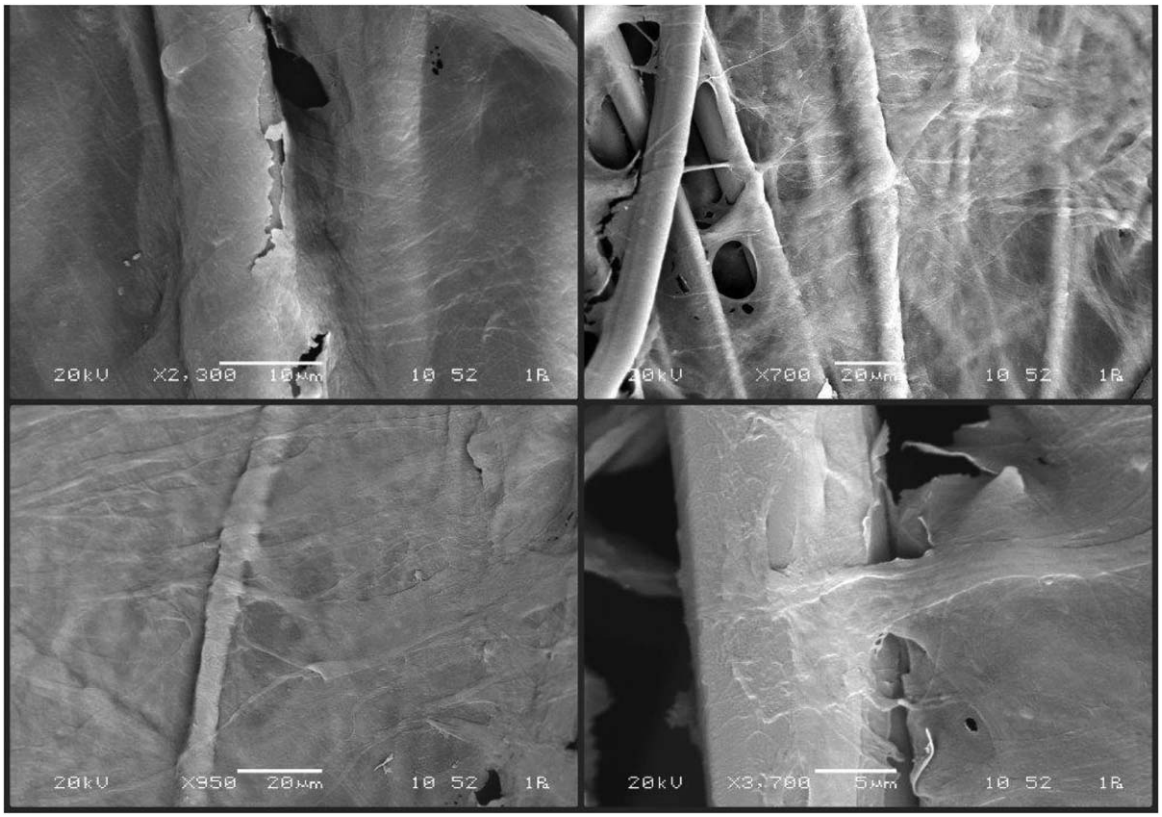


**Figure 5.** Scanning electron microphotographs of SF1 after 14 days of ASC culture at different magnifications.

during time, but this effect is more evident at day 14 in presence of PL (Figure 4).

When ASCs were cultured for 14 days on SF1, both abundant extracellular matrix and adhered cells could be appreciated (Figure 5). The cells migrated inside the scaffold and colonized it by using their cytoplasmic extensions. Notwithstanding its compactness, the mat porosity seems to be optimal to host expanding cell clusters.

The characteristic fibroblast-like shape of ASCs could be observed in the TEM microphotographs [Figure 6(a)]; the overall cytoplasmic pattern is typical for fully active cells, cell membrane appears continuous, regular and well delimited, except for some indented regions. Several vesicles with a non-homogeneous, granular content are present in the cytoplasm: four of them are visible in close proximity of the plasmalemma [Figure 6(a)], where an active exocytosis process could be speculated, since the vesicles are located near the indented margins. A network of rough endoplasmic reticulum can be observed, mainly at higher magnifications [Figure 6(a–c)]. The cell-scaffold space is minimal and interrupted by adherence zonulae, where a real interface can be identified [Figure 6(b,c)].

### *In Vivo* Results

Epithelial/dermal wounds were carry out on the dorsal surface of 10 rabbits; SF1 scaffolds soaked with PL alone (group 1, $n = 4$) or associated with ASCs (group 2, $n = 4$) were applied; finally group 3 (control, $n = 2$) was treated with silk fibroin soaked with sterile physiological solution. Each scaffold was changed every 72 h, with the same composition and dosage, for a total of three applications. Figure 7 reports representative images of the wounds healing process as a function of time.

During the experiments, animals did not present inflammatory symptoms and no fever or pain was noticed. No bacterial infection was identified and the wound resolution gave rise to different outcomes. In fact, it has been possible to demonstrate three different evolution of the tissue (Figure 7). In general, animals either of group 1 or group 2 demonstrated a satisfactory tissue regeneration, in fact they did not show any adverse reaction, no pain or itch was detected (Figure 7). In detail, a complete reparation process was observed 9 days after the lesion in animals treated with SF1 and PL (group 1); 72 h after lesion event (day 3), an intensive proliferative activity was observed; absence of seroma, no inflammatory signs and no scar itch were highlighted. At day 6, the lesion area was entirely repaired and just a mild reddening was set forth (Figure 7). Rabbits treated with SF1 associated with ASCs and PL (group 2), presented a reparative tissue process characterized by granulation process (platelet aggregation) at day 3 after the lesion event; the surrounding tissue did not present inflammatory signs, in fact no swelling, oedema, or other symptoms were observed. At day 6 the whole regenerative course was evaluated, highlighting a further tissue organization, and finally, at day 9 the scar was completely substituted by a regenerated epithelium characterized by a mild and thin scarring tissue. Despite at day 3 the lesion appeared particularly critical with respect to group 1, characterized by the scar formation, a complete anatomical reorganization of the

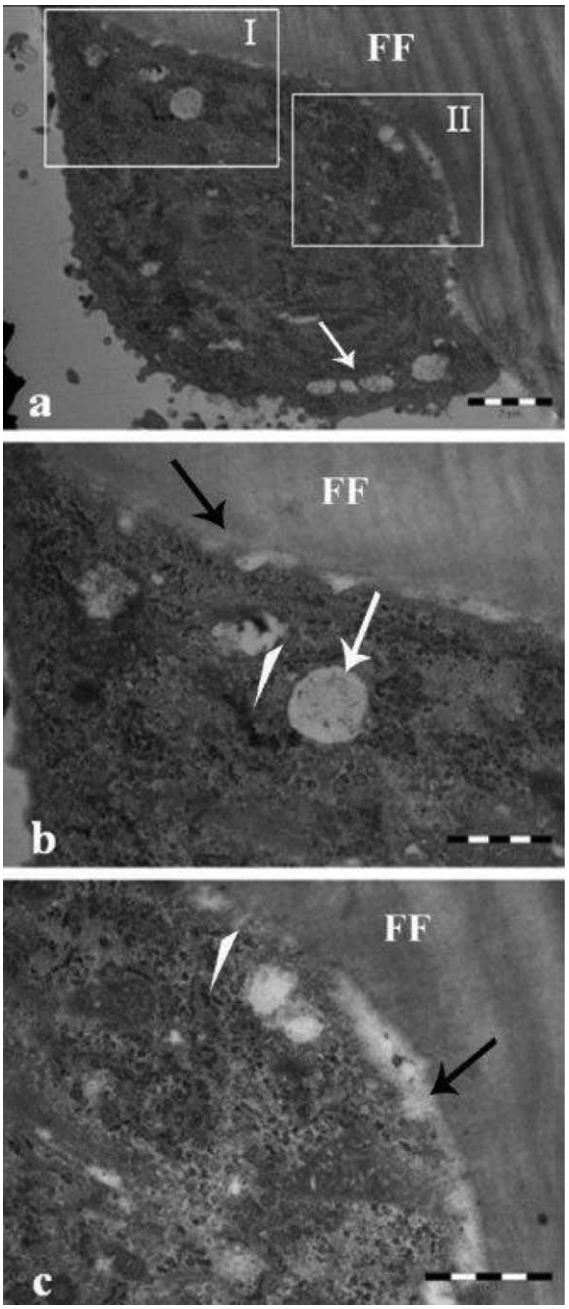


**Figure 6.** Transmission electron microphotograph of ASCs after 14 days of culture (a). The insets I and II in figure (a) are magnified in figures b and c, respectively. FF: fibroin fibers; White arrows: vesicles; black arrow: cell-fibroin fibers interface; white arrowheads: rough endoplasmic reticule. Bars in figure a: 2 μm; bars in figures b and c: 1 μm.

epithelium was observed at day 9 when the scar formation was removed. Animals treated with SF1 alone (group 3) demonstrated a classical reparation evolution at day 3, based on clotting cascade and granulation phase (inflammatory process). In particular, an initial regenerative process in the peripheral area was notice and a granulation phase with proud flesh evidence was observed in the central area. Reparative evolution developed slowly, swelling and mild edema in the lesion core was observed. Finally, at day 9, the wound was not completely repaired, in fact the surrounding area presented itch and the middle zone was not re-epithelized. The inflammatory process was totally restored and signs of secondary infection were absent. Furthermore, rabbits felt uncomfortable, they did not exhibit pain, but compliant sensation caused by the scar itch (Figure 7).

Each photograph (10 rabbits for three time points, $n = 30$) was examined by three independent expert operators, and a score between 10 (no difference from starting wound) and 0 (complete wound healing) was attributed. ANOVA analysis evidenced that both treatment and time have a significant effect on wound healing (mean $\pm$ st. dev.: $3.06 \pm 2.221$ for group 1; $5.61 \pm 2.893$ for group 2; $4.00 \pm 1.936$ for group 3; $P \leq 0.0001$). In particular, a wound reduction was detected for all treatment groups during time; at day 3 and 6 no differences were observed between animals treated with or without PL (group 1 and group 3), while the wound healing was significantly slower in animals treated with ASCs and PL (group 2) (Figure 8).

At the end of procedures, the combination of fibroin nonwoven mats and PL significant improved the wound healing process (Figure 8).

## DISCUSSION

In this work, silk fibroin nonwoven mats were obtained by a large scale water entanglement method, this method could also refer to the spunlace or hydroentanglement technique for the production of nonwoven fabrics. At the best of our knowledge no other examples in literature are reported regarding the use of this technique applied to the production of biomaterials. The use of this method, with respect to other commonly applied techniques for the obtainment of scaffolds, sponges or other materials for biomedical applications such as electrospinning or salt leaching from crosslinked hydrogels, shows several advantages. For example, in common polymer processing techniques, different organic solvents are required to bring the polymer in solution, in the case of our fibroin based materials only water is used and the polymer, being a natural fiber, does not require any solubilization but only some carding procedure which could be economically performed by an industrial equipment. In this way, also the production translation to the industry is favored and the scale-up easily affordable. This is of enormous importance if compared to, e.g., electrospinning that requires expansive equipment and does not allow large scale productions at reasonable costs. All these aspects reduce also the ecologic concerns. Furthermore, by a biomedical point of view, it is known that obtaining nonwoven fabrics by the water entanglement method, allows the formation of materials with optimal air permeability, usually higher with respect to other methods for obtaining nonwoven mats. This is a fundamental aspect when the mat is placed on the wound, because the oxygen is fundamental in the healing process.[72]

Silk fibroin nonwoven mats were characterized in term of weight/area ratio, thickness and porosity % (Table I): porosity, that is one of the most important parameters for cell attachment and proliferation, is almost the same for all the specimens indicating that, probably, independently from the sample

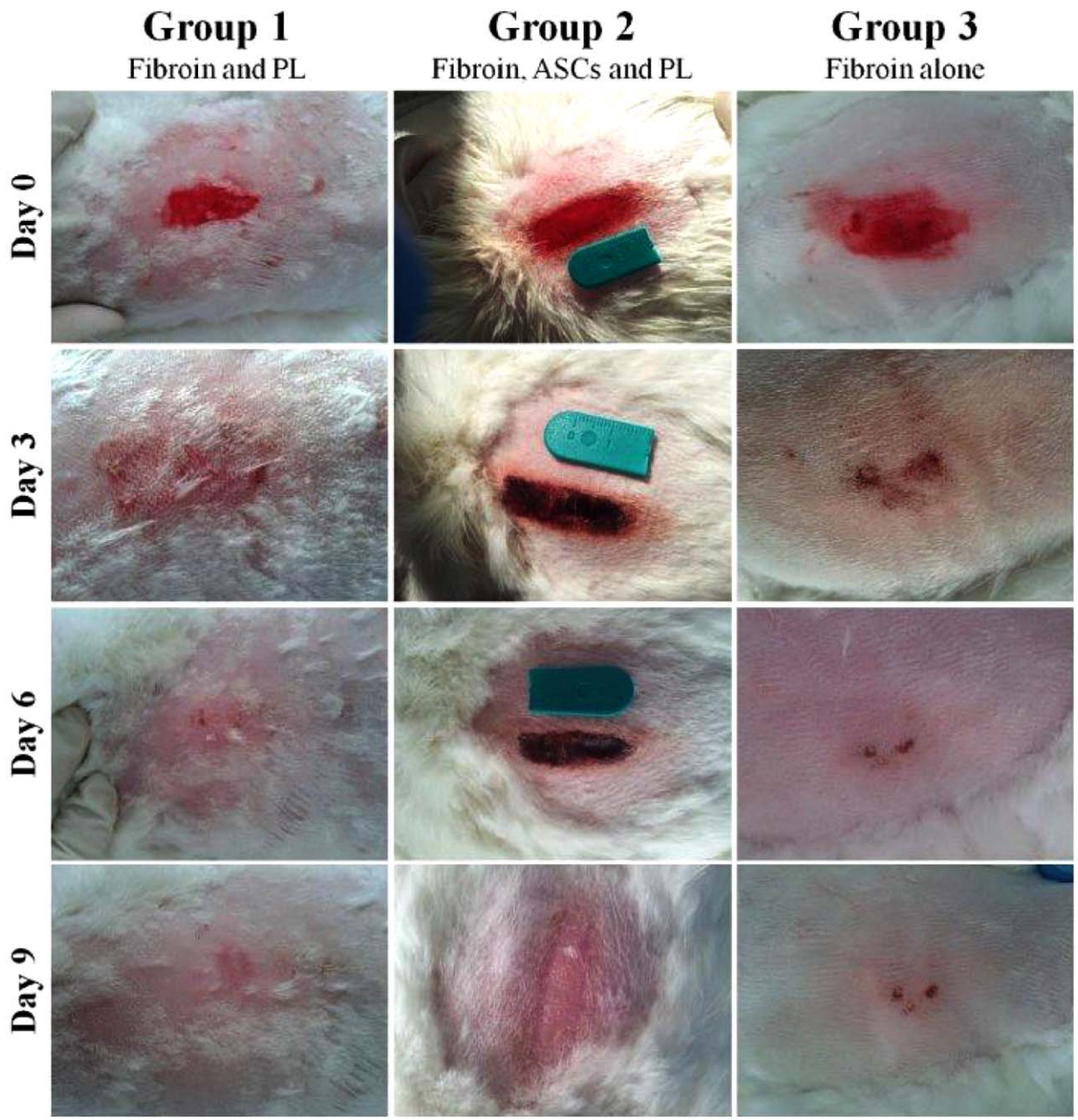


**Figure 7.** Photographs of the wounds taken at postoperative days 0, 3, 6, and 9. Group 1 ($n = 4$) was treated with SF1 soaked with PL alone, group 2 ($n = 4$) with SF1 and ASCs diluted in PL, group 3 ($n = 2$) was treated with SF1 soaked with physiological solution. Each scaffold was changed every 72 h, with the same composition and dosage, for a total of three applications. [Color figure can be viewed in the online issue, which is available at wileyonlinelibrary.com.]

thickness, all the obtained materials could be proposed for the *in vivo* application. The high porosity shown by the obtained SF mats by the water entanglement method results higher than that obtained by similar nonwoven mats produced by electrospinning.[30] The results from optical photography (Figure 1) supports these data giving an experimental evidence that the water entanglement method could be suitable in tailoring the main macroscopic characteristics of the material still maintaining constant porosity and spatial orientation of the fibers. The SEM investigation indicates an optimized mat production process (Figure 2): scaffolds, macroscopically different in terms of thickness are undistinguishable by SEM; the mats result in different weight and thickness, but similar in texture and porosity. Moreover, but not less important, SEM investigation evidences the absence of sericin on fibroin fibers, confirming the suitability of the sericin extraction method. The structure of fibroin mats used in our study seems to be similar to that obtained with electrospinning technology by Jeong *et al.* (2014),[73] but differently from electrospinning it looks more simple to achieve mats with tailorable and reproducible

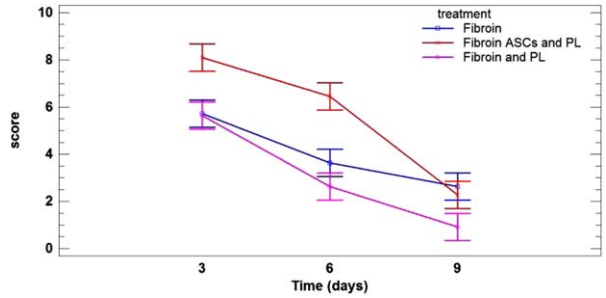


**Figure 8.** Mean values and 95.0% LSD intervals of scores during time for each treatment group. [Color figure can be viewed in the online issue, which is available at wileyonlinelibrary.com.]

macroscopic behaviors by using the water entanglement method because structural and mechanical properties of mats can be modulated by simple modification of the production apparatus setting.[74]

FTIR analysis of fibroin nonwoven mat presents peaks at 1626 and 1518 $cm^{-1}$, respectively for Amide I and Amide II [Figure 3(A), red line]. These bands indicate that the applied processing method does not modify the original secondary structure of silk fibroin. Similar results were obtained by Dal Pra *et al.* (2003), a silk fibroin nonwoven 3D scaffold presents bands at 1620 and 1516 $cm^{-1}$, attributed to $\beta$-sheet structure.[32]

SF1 scaffolds were sterilized by autoclaving or with gamma rays. All of these stand the sterility test by BacT/ALERT 3D system. In literature the sterilization of fibroin-based materials is often performed by autoclaving.[75–79] Lawrence *et al.* (2008) observed that after steam sterilization, silk fibroin films presented FTIR peaks shifted to lower wavenumbers, indicating a $\beta$-sheet increase.[67] Kojthung *et al.* (2008) gamma-irradiated silk fibroin fibers (up to 3000 kGy) and indicated that $\gamma$-rays did not act on primary structure of protein, but induced a faster biodegradation.[80] Furthermore, Byun *et al.* (2010) observed an antitumor potentiality of gamma-irradiated silk fibroin solution (up to 200 kGy).[81] The results from FTIR analysis before sterilization performed on sample SF1, indicate that sterilization does not induce fibroin conformation change. DSC analysis confirmed FTIR findings: before and after sterilization, SF1 scaffold presents an endothermic peak related to fibroin degradation at ~320°C [Figure 3(B)], confirming previous observations.[82]

The mechanical properties of SF1 and SF3 were evaluated in terms of tensile strength and elongation at break. These experiments were performed as a function of sample orientation: parallel orientation means that the tensile force direction follows the same orientation of the fibers as obtained from carding/combing machine, while perpendicular orientation indicates that the tensile force direction has been applied perpendicularly to the fiber orientation. The fiber mat orientation and mat thickness show a significant effect on mechanical properties. In fact, the sample SF1, that is the thinnest, shows a tensile strength, in parallel orientation, 32% lower than SF3 mat, while elongation at break results similar. This result could be justified by the fact that applying the tensile force along the fiber orientation further aligned the fibers and the resulting tensile strength results strictly related to intrinsic fibroin mechanical properties. Furthermore, the absolute magnitude of the effect resulted also related to the sample thickness. When the tensile force is applied perpendicularly to the fiber orientation the mechanical behaviors worsen due to the de-entanglement of the fibers under the mechanical force.

A common example of this phenomenon is given by a normal rope, if the mechanical stress is applied parallel to the rope-fiber orientation the rope will resist otherwise it will de-entangle. In the worst hypothesis of a perpendicular mechanical stress applied to the mats, a tensile strength ranging 0.99–1.30 MPa, as found for SF1 and SF3, could be considered more than sufficient for applications on wounds.

On the basis of the technological and mechanical properties, SF1 was selected for the further *in vitro* and *in vivo* analyses. Silk fibroin nonwoven mat supports cell adhesion and proliferation: due to scaffold porosity, ASCs are able to migrate inside the scaffold and colonize it. Moreover, the presence of PL improves the cell proliferation (Figure 4). For all these reasons, we used SF1 to evaluate its capacity to improve wound healing in an animal model. In addition, for the first time we considered the *in vivo* effect of PL on silk fibroin scaffold in combination with ASCs. A complete wound healing process was observed in animals treated with PL; the combined use of PL and ASCs induced a reparative tissue process characterized by platelet aggregation, mainly observed after 3 days of treatment, but a complete anatomical re-organization of epithelium was observed at day 9. ASCs show positive effects on wound healing *in vivo*[83] because they enhance neovascularization,[84,85] release bioactive substances (e.g., proangiogenic factors) and have differentiative potential[86]; however our results indicated a more pronounced effect on wound healing using PL alone. After 9 days of application on rabbit wounds, a complete re-epithelization has been observed for the fibroin scaffolds containing PL, but not for fibroin scaffolds alone. This result seems to suggest an increase in reparative process when scaffold was applied together with one of the two considered biologicals.

By comparing our results with other works, which propose similar approaches with similar aims, it could be possible to evidence some advantage in terms of wound healing ability of the processed fibroin with respect to different techniques other than the here proposed water entanglement method. For example, Navone *et al.* tested a silk fibroin patch, obtained by electrospinning, on a murine wound healing model. Scaffold were used alone or combined to ASCs. Also taking into consideration that the animal model and type of scaffold are different from ours, the time of healing for our combination of SF with PL looks faster.[54] A similar outcome could be found in Pelizzo *et al.* that have recently proposed the use of mesenchymal stem cells suspension for the regeneration of cutaneous lesion in rabbit model. The cells, directly injected into the wound bed, have accelerated the wound healing process; on the other hand, scar was observed till 11 days after treatment.[87] In another study, Jeong *et al.* prepared nanofibrous matrices containing silver sulfadiazine (SSD) wound dressings.[73] Similarly to our study, the fibroin material alone shown some effect in wound healing in

14 days while using silver sulfadiazine in combination with fibroin mats brought to a faster healing of the wound. It looks that at day 9 that is the time we observed for the *restitutio ad integrum* of the animals treated with the combination SF/PL, the study from Jeong showed a less impressive impact in the wound resolution. Similar considerations could arise from comparing the present work with other papers using comparable approaches.[88]

To conclude, the combined use of tridimensional fibroin scaffold obtained by an innovative (for biomaterials) water entanglement technique and cellular components (PL/ASCs) allowed us to speed up healing and scar disappearance. Of course, this method for the production of non-woven mats could be extended to a number of applications and could open a new way in the processing of polymer based biomaterials.

## CONCLUSION

Nonwoven silk fibroin mats have been obtained by a water entanglement method allowing the production of three different scaffolds. The samples resulted in different weight/area ratio, but showed similar porosity and fiber orientation. The thinnest scaffold was used for the *in vitro* analysis and *in vivo* wound healing evaluation on rabbit due to its greater easy of handle with respect to the other two thicker samples. Adipose-derived stromal cells were able to adhere, migrate, and proliferate inside the fibroin nonwoven mat and platelet lysate improved the cell growth.

*In vivo*, the use of platelet lysate on silk fibroin scaffold demonstrated the potential of this biomaterial for regenerative medicine applications. In particular, the fibroin mat could act as a mechanical support in order to guarantee the correct interaction between the bioactive substances and the degenerated tissue without adverse reactions (inflammatory/allergic response) in the *in vivo* model.

## ACKNOWLEDGMENTS

This work was supported by Fondazione Cariplo (FIBROPAN, Project Id. 2012-0878), and by Fondazione Cariplo and Regione Lombardia (STEMDELIVERY, Project Id. 42617604). The authors thank Sanitars S.p.a (Flero, Italy), Gammatom S.r.l. (Guanzate, Italy) for scaffold sterilization, and Dr V. Necchi (Centro Grandi Strumenti, Pavia University, Italy) for the ultrastructural investigation. Mrs A. Ghizzardi, and Dr. D. Pedretti's skilful technical assistance is gratefully acknowledged.

## AUTHOR CONTRIBUTIONS

M.L. Torre, M. Ferrari, S. Faragò and M. Marazzi conceived the work and designed the experiments; S. Perteghella, B. Vigani, B. Crivelli, S. Renzi, S. Dotti and A. Boschi performed the experiments; T. Chlapanidas, G. Tripodo, S. Preda and M. L.Torre analyzed the data and wrote the article.

## REFERENCES

1. Greaves, N. S.; Iqbal, S. A.; Baguneid, M.; Bayat, A. *Wound Repair Regen.* **2013**, *21*, 194.
2. Palumbo, F. S.; Pitarresi, G.; Mandracchia, D.; Tripodo, G.; Giammona, G. *Carbohydr. Polym.* **2006**, *66*, 379.
3. Pitarresi, G.; Pierro, P.; Palumbo, F. S.; Tripodo, G.; Giammona, G. *Biomacromolecules* **2006**, *7*, 1302.
4. Tripodo, G.; Wischke, C.; Neffe, A. T.; Lendlein, A. *Carbohydr. Res.* **2013**, *381*, 59.
5. Pitarresi, G.; Palumbo, F. S.; Tripodo, G.; Cavallaro, G.; Giammona, G. *Eur. Polym. J.* **2007**, *43*, 3953.
6. Mogosanu, G. D.; Grumezescu, A. M. *Int. J. Pharma.* **2014**, *463*, 127.
7. Tripodo, G.; Wischke, C.; Lendlein, A.; Materials, R.; Society, S. *Proceedings* **2012**, *1403*, 21.
8. Tripodo, G.; Wischke, C.; Lendlein, A. *Macromol. Symp.* **2011**, *309310*, 49.
9. Wischke, C.; Tripodo, G.; Choi, N. Y.; Lendlein, A. *Macromol. Biosci.* **2011**, *11*, 1637.
10. Innocente, F.; Mandracchia, D.; Pektok, E.; Nottelet, B.; Tille, J. C.; de Valence, S.; Faggian, G.; Mazzucco, A.; Kalangos, A.; Gurny, R.; Moeller, M.; Walpoth, B. H. *Circulation* **2009**, *120*, S37.
11. Nottelet, B.; Pektok, E.; Mandracchia, D.; Tille, J. C.; Walpoth, B.; Gurny, R.; Moller, M. *J. Biomed. Mater. Res. Part A* **2009**, *89A*, 865.
12. Nottelet, B.; Mandracchia, D.; Gurny, R.; Moller, M.; Pektok, E.; Walpoth, B. H. *Int. J. Artif. Org.* **2007**, *30*, 706.
13. Malafaya, P. B.; Silva, G. A.; Reis, R. L. *Adv. Drug Deliv. Rev.* **2007**, *59*, 207.
14. Sobajo, C.; Behzad, F.; Yuan, X. F.; Bayat, A. *Eplasty* **2008**, *8*, e47.
15. Gu, Z.; Xie, H.; Huang, C.; Li, L.; Yu, X. *Int. J. Biol. Macromol.* **2013**, *58*, 121.
16. Kanokpanont, S.; Damrongsakkul, S.; Ratanavaraporn, J.; Aramwit, P. *Int. J. Pharma.* **2012**, *436*, 141.
17. Karahaliloğlu, Z.; Ercan, B.; Denkbaş, E. B.; Webster, T. J. *J. Biomed. Mater. Res. A* **2014**, *103*, 135.
18. Luangbudnark, W.; Viyoch, J.; Laupattarakasem, W.; Surakunprapha, P.; Laupattarakasem, P. *Sci. World J.* **2012**, *2012*, 697201.
19. Vasconcelos, A.; Gomes, A. C.; Cavaco-Paulo, A. *Acta Biomater.* **2012**, *8*, 3049.
20. Zhang, R.; Liu, Y.; Yan, K.; Chen, L.; Chen, X. R.; Li, P.; Chen, F. F.; Jiang, X. D. *J. Neuroinflamm.* **2013**, *10*, 106.
21. Vepari, C.; Kaplan, D. L. *Prog. Polym. Sci.* **2007**, *32*, 991.
22. Kim, U. J.; Park, J.; Kim, H. J.; Wada, M.; Kaplan, D. L. *Biomaterials* **2005**, *26*, 2775.
23. Jin, H. J.; Chen, J. S.; Karageorgiou, V.; Altman, G. H.; Kaplan, D. L. *Biomaterials* **2004**, *25*, 1039.
24. Cai, Z.; Mo, X.; Zhang, K.; Fan, L.; Yin, A.; He, C.; Wang, H. *S. Int. J. Mol. Sci.* **2010**, *11*, 3529.
25. Chlapanidas, T.; Farago, S.; Mingotto, F.; Crovato, F.; Tosca, M. C.; Antonioli, B.; Bucco, M.; Lucconi, G.; Scalise, A.; Vigo, D.; Faustini, M.; Marazzi, M.; Torre, M. L. *Tissue Eng. Part A* **2011**, *17*, 1725.
26. Chlapanidas, T.; Tosca, M. C.; Farago, S.; Perteghella, S.; Galuzzi, M.; Lucconi, G.; Antonioli, B.; Ciancio, F.;

Rapisarda, V.; Vigo, D.; Marazzi, M.; Faustini, M.; Torre, M. L. *Int. J. Immunopathol. Pharmacol.* **2013**, *26*, 43.

27. Faragò, S.; Lucconi, G.; Perteghella, S.; Vigani, B.; Tripodo, G.; Sorrenti, M.; Catenacci, L.; Boschi, A.; Faustini, M.; Vigo, D.; Chlapanidas, T.; Marazzi, M.; Torre, M. L. Pharma. Dev. Technol **2015**, *11*, 1.
28. Unger, R. E.; Peters, K.; Wolf, M.; Motta, A.; Migliaresi, C.; Kirkpatrick, C. J. *Biomaterials* **2004**, *25*, 5137.
29. Unger, R. E.; Wolf, M.; Peters, K.; Motta, A.; Migliaresi, C.; Kirkpatrick, C. J. *Biomaterials* **2004**, *25*, 1069.
30. Min, B. M.; Lee, G.; Kim, S. H.; Nam, Y. S.; Lee, T. S.; Park, W. H. *Biomaterials* **2004**, *25*, 1289.
31. Bray, L. J.; George, K. A.; Hutmacher, D. W.; Chirila, T. V.; Harkin, D. G. *Biomaterials* **2012**, *33*, 3529.
32. Dal Pra, I.; Petrini, P.; Charini, A.; Bozzini, S.; Fare, S.; Armato, U. *Tissue Eng.* **2003**, *9*, 1113.
33. Kasoju, N.; Bhonde, R. R.; Bora, U. *J. Tissue Eng. Regen. Med.* **2009**, *3*, 539.
34. Schellenberg, A.; Ross, R.; Abagnale, G.; Joussen, S.; Schuster, P.; Arshi, A.; Pallua, N.; Jockenhoevel, S.; Gries, T.; Wagner, W. *Plos One* **2014**, *9*, e94353.
35. Lu, L. X.; Zhang, X. F.; Wang, Y. Y.; Ortiz, L.; Mao, X.; Jiang, Z. L.; Xiao, Z. D.; Huang, N. P. *ACS Appl. Mater. Interfaces* **2013**, *5*, 319.
36. Shen, L.; Zeng, W.; Wu, Y. X.; Hou, C. L.; Chen, W.; Yang, M. C.; Li, L.; Zhang, Y. F.; Zhu, C. H. *Cell Transplant.* **2013**, *22*, 1011.
37. Hodgkinson, T.; Bayat, A. *Arch. Dermatol. Res.* **2011**, *303*, 301.
38. Pajardi, G.; Rapisarda, V.; Somalvico, F.; Scotti, A.; Russo, G. L.; Ciancio, F.; Sgrò, A.; Nebuloni, M.; Allevi, R.; Torre, M. L.; Trabucchi, E.; Marazzi, M. *Int. Wound J.* **2014**. doi: 10.1111/iwj.12223.
39. Kamel, R. A.; Ong, J. F.; Eriksson, E.; Junker, J. P. E.; Caterson, E. J. *J. Am. Coll. Surg.* **2013**, *217*, 533.
40. Zahorec, P.; Koller, J.; Danisovic, L.; Bohac, M. *Cell Tissue Bank.* **2014**, *15*, 641.
41. Bourin, P.; Bunnell, B. A.; Casteilla, L.; Dominici, M.; Katz, A. J.; March, K. L.; Redl, H.; Rubin, J. P.; Yoshimura, K.; Gimble, J. M. *Cytotherapy* **2013**, *15*, 641.
42. Faustini, M.; Bucco, M.; Chlapanidas, T.; Lucconi, G.; Marazzi, M.; Tosca, M. C.; Gaetani, P.; Klinger, M.; Villani, S.; Ferretti, V. V.; Vigo, D.; Torre, M. L. *Tissue Eng. Part C Methods* **2010**, *16*, 1515.
43. Gaetani, P.; Torre, M. L.; Klinger, M.; Faustini, M.; Crovato, F.; Bucco, M.; Marazzi, M.; Chlapanidas, T.; Levi, D.; Tancioni, F.; Vigo, D.; Rodriguez y Baena, R. *Tissue Eng. A* **2008**, *14*, 1415.
44. Ghidoni, I.; Chlapanidas, T.; Bucco, M.; Crovato, F.; Marazzi, M.; Vigo, D.; Torre, M. L.; Faustini, M. *Cytotechnology* **2008**, *58*, 49.
45. Wilson, A.; Butler, P. E.; Seifalian, A. M. *Cell Proliferat.* **2011**, *44*, 86.
46. Mizuno, H. *Curr. Opin. Mol. Therap.* **2010**, *12*, 442.
47. Marazzi, M.; Crovato, F.; Bucco, M.; Sironi, M. C.; Tosca, M. C.; Antonioli, B.; Chlapanidas, T.; Lucconi, G.; Rapisarda, V.; Scalise, A.; Vigo, D.; Faustini, M.; Torre, M. L. *Cell Transplant.* **2012**, *21*, 373.
48. Folgiero, V.; Migliano, E.; Tedesco, M.; Iacovelli, S.; Bon, G.; Torre, M. L.; Sacchi, A.; Marazzi, M.; Bucher, S.; Falcioni, R. *Cell Transplant.* **2010**, *19*, 1225.
49. Renzi, S.; Ricco, S.; Dotti, S.; Sesso, L.; Grolli, S.; Cornali, M.; Carlin, S.; Patruno, M.; Cinotti, S.; Ferrari, M. *Res. Vet. Sci.* **2013**, *95*, 272.
50. de Girolamo, L.; Lucarelli, E.; Alessandri, G.; Avanzini, M. A.; Bernardo, M. E.; Biagi, E.; Brini, A. T.; D'Amico, G.; Fagioli, F.; Ferrero, I.; Locatelli, F.; Maccario, R.; Marazzi, M.; Parolini, O.; Pessina, A.; Torre, M. L. *Italian Mesenchymal Stem Cell G. Curr. Pharma. Des.* **2013**, *19*, 2459.
51. Markeson, D.; Pleat, J. M.; Sharpe, J. R.; Harris, A. L.; Seifalian, A. M.; Watt, S. M. *J. Tissue Eng. Regen. Med.* **2013**, *9*, 649.
52. Altman, A. M.; Yan, Y.; Matthias, N.; Bai, X.; Rios, C.; Mathur, A. B.; Song, Y. H.; Alt, E. U. *Stem Cells* **2009**, *27*, 250.
53. Tripodo, G.; Chlapanidas, T.; Perteghella, S.; Vigani, B.; Mandracchia, D.; Trapani, A.; Galuzzi, M.; Tosca, M. C.; Antonioli, B.; Gaetani, P.; Marazzi, M.; Torre, M. L. *Colloids Surf. B Biointerfaces* **2015**, *125*, 300.
54. Navone, S. E.; Pascucci, L.; Dossena, M.; Ferri, A.; Invernici, G.; Acerbi, F.; Cristini, S.; Bedini, G.; Tosetti, V.; Ceserani, V.; Bonomi, A.; Pessina, A.; Freddi, G.; Alessandrino, A.; Ceccarelli, P.; Campanella, R.; Marfia, G.; Alessandri, G.; Parati, E. A. *Stem Cell Res. Ther.* **2014**, *5*, 7.
55. Bieback, K. *Transfusion Med. Hemother.* **2013**, *40*, 326.
56. Barsotti, M. C.; Losi, P.; Briganti, E.; Sanguinetti, E.; Magera, A.; Al Kayal, T.; Feriani, R. D.; Stefano, R.; Soldani, G. *Plos One* **2013**, *8*, e84753.
57. Ranzato, E.; Patrone, M.; Mazzucco, L.; Burlando, B. *Br. J. Dermatol.* **2008**, *159*, 537.
58. El Backly, R.; Ulivi, V.; Tonachini, L.; Cancedda, R.; Descalzi, F.; Mastrogiacomo, M. *Tissue Eng. A* **2011**, *17*, 1787.
59. Cipriani, V.; Ranzato, E.; Balbo, V.; Mazzucco, L.; Cavaletto, M.; Patrone, M. *J. Tissue Eng. Regen. Med.* **2009**, *3*, 531.
60. Mori, M.; Rossi, S.; Bonferoni, M. C.; Ferrari, F.; Sandri, G.; Riva, F.; Del Fante, C.; Perotti, C.; Caramella, C. *Int. J. Pharma.* **2014**, *461*, 505.
61. Rossi, S.; Faccendini, A.; Bonferoni, M. C.; Ferrari, F.; Sandri, G.; Del Fante, C.; Perotti, C.; Caramella, C. M. *Int. J. Pharma.* **2013**, *440*, 207.
62. Dozza, B.; Di Bella, C.; Lucarelli, E.; Giavaresi, G.; Fini, M.; Tazzari, P. L.; Giannini, S.; Donati, D. *J. Orthopaed. Res.* **2011**, *29*, 961.
63. Faragò, S.; Lorenzotti, L. Italian patent application ITMI20080500 (A1), Italy: **2008**.
64. Chlapanidas, T.; Farago, S.; Lucconi, G.; Perteghella, S.; Galuzzi, M.; Mantelli, M.; Avanzini, M. A.; Tosca, M. C.; Marazzi, M.; Vigo, D.; Torre, M. L.; Faustini, M. *Int. J. Biol. Macromol.* **2013**, *58*, 47.
65. Vaz, C. M.; van Tuijl, S.; Bouten, C. V. C.; Baaijens, F. P. T. *Acta Biomater.* **2005**, *1*, 575.

66. Chen, X.; Shao, Z. Z.; Marinkovic, N. S.; Miller, L. M.; Zhou, P.; Chance, M. R. *Biophys. Chem.* **2001**, *89*, 25.

67. Lawrence, B. D.; Omenetto, F.; Chui, K.; Kaplan, D. L. *J. Mater. Sci.* **2008**, *43*, 6967.

68. Um, I. C.; Kweon, H. Y.; Park, Y. H.; Hudson, S. *Int. J. Biol. Macromol.* **2001**, *29*, 91.

69. Vasconcelos, A.; Freddi, G.; Cavaco-Paulo, A. *Biomacromolecules* **2008**, *9*, 1299.

70. Luengo Gimeno, F.; Gatto, S.; Ferro, J.; Croxatto, J. O.; Gallo, J. E. *Thromb. J.* **2006**, *4*, 18.

71. Zhang, K.; Qian, Y.; Wang, H.; Fan, L.; Huang, C.; Yin, A.; Mo, X. *J. Biomed. Mater. Res. A* **2010**, *95A*, 870.

72. Midha, V. K.; Dakuri, A.; Midha, V. *J. Ind. Text.* **2013**, *43*, 174.

73. Jeong, L.; Kim, M. H.; Jung, J. Y.; Min, B. M.; Park, W. H. *Int. J. Nanomed.* **2014**, *9*, 5277.

74. Hajiani, F.; Hosseini, S. M.; Ansari, N.; Jeddi, A. A. A. *Fibers Polym.* **2010**, *11*, 798.

75. Meinel, L.; Hofmann, S.; Karageorgiou, V.; Zichner, L.; Langer, R.; Kaplan, D.; Vunjak-Novakovic, G. *Biotechnol. Bioeng.* **2004**, *88*, 379.

76. Gellynck, K.; Verdonk, P. C. M.; Van Nimmen, E.; Almqvist, K. F.; Gheysens, T.; Schoukens, G.; Van Langenhove, L.; Kiekens, P.; Mertens, J.; Verbruggen, G. *J. Mater. Sci. Mater. Med.* **2008**, *19*, 3399.

77. Wang, Y. Z.; Blasioli, D. J.; Kim, H. J.; Kim, H. S.; Kaplan, D. L. *Biomaterials* **2006**, *27*, 4434.

78. Mauney, J. R.; Nguyen, T.; Gillen, K.; Kirker-Head, C.; Gimble, J. M.; Kaplan, D. L. *Biomaterials* **2007**, *28*, 5280.

79. Hofmann, S.; Hagenmueller, H.; Koch, A. M.; Mueller, R.; Vunjak-Novakovic, G.; Kaplan, D. L.; Merkle, H. P.; Meinel, L. *Biomaterials* **2007**, *28*, 1152.

80. Kojthung, A.; Meesilpa, P.; Sudatis, B.; Treeratanapiboon, L.; Udomsangpetch, R.; Oonkhanond, B. *Int. Biodeteriorat. Biodegrad.* **2008**, *62*, 487.

81. Byun, E. B.; Sung, N. Y.; Kim, J. H.; Choi, J.; Matsui, T.; Byun, M. W.; Lee, J. W. *Chem. Biol. Interact.* **2010**, *186*, 90.

82. Nakamura, S.; Saegusa, Y.; Yamaguchi, Y.; Magoshi, J.; Kamiyama, S. *J. Appl. Polym. Sci.* **1986**, *31*, 955.

83. Shingyochi, Y.; Orbay, H.; Mizuno, H. Expert Opin. Biol. Ther. **2015**, *15*, 1285. doi: 10.1517/14712598.2015.1053867.

84. Nie, C.; Yang, D.; Xu, J.; Si, Z.; Jin, X.; Zhang, J. *Cell Transplant.* **2011**, *20*, 205.

85. Wu, Y.; Chen, L.; Scott, P. G.; Tredget, E. E. *Stem Cells* **2007**, *25*, 2648.

86. Fu, X.; Li, H. *Cell Tissue Res.* **2009**, *335*, 317.

87. Pelizzo, G.; Avanzini, M. A.; Cornaglia, A. I.; Osti, M.; Romano, P.; Avolio, L.; Maccario, R.; Dominici, M.; De Silvestri, A.; Andreatta, E.; Costanzo, F.; Mantelli, M.; Ingo, D.; Piccinno, S.; Calcaterra, V. *J. Transl. Med.* **2015**, *13*, 219.

88. Motealleh, B.; Zahedi, P.; Rezaeian, I.; Moghimi, M.; Abdolghaffari, A. H.; Zarandi, M. A. *J. Biomed. Mater. Res. B Appl. Biomater.* **2014**, *102*, 977.